COMPUTATION OF TRANSONIC FLOW WITH DETACHED BOW SHOCKS THROUGH TWO-DIMENSIONAL TURBOMACHINERY CASCADES

F.G. SATOR
Institut d'Aérodynamique
Ecole Polytechnique Fédérale
de Lausanne, Suisse

Abstract

A method is presented for computing steady inviscid transonic flows with and without detached bow-shocks in turbomachinery cascades, wherein both subsonic and supersonic regions co-exist. A finite difference method based on the small disturbance formulation of the non-linear problem is used. Different finite difference equations which are appropriate to the behaviour of the differential equation at each mesh point are formulated. Weak shock structures are permitted to develop as a part of the solution process, without prior knowledge of their exact strength and position.

To take into account viscous effects, the displacement thickness of the boundary layer is added to the blade contour.

A variation of the basic procedure is used to solve the inverse problem to design airfoil contours for given pressure distribution.

The computed surface pressure distributions for given airfoil shapes agree well with experimental results.

Introduction

The design and development of turbomachineries require three-dimensional solution to the flow field internal to rotating and stationary cascades. 1950, Wu proposed to solve the flow equations on seperate orthogonal quasi-two-dimensional surfaces in space.[1] Solution techniques suitable for the S2 (radially oriented surfaces) appeared rather quickly. The blade-to-blade solutions have been achieved somewhat more slowly. A subsonic relaxation technique utilizing the stream function equation was proposed by Wu and developed by Katsanis and McNally.[2] The difficulty of this approach lies in the restriction to uniformly subsonic Mach numbers and that the reduction of derivatives of stream function to velocities and densities is double-valued with Mach number. No such ambiguity arises if the dependent variable is selected to be the velocity potential. Murman and Cole developed a relaxation technique capable of rapidly and efficiently handling local areas of supersonic flow around isolated airfoils.[4] The method is based on the realization that one must vary the difference star to match the characteristics of the governing differential equations. Dodge used this technique to predict deviation angles and optimum angles of attack for cascades in transonic flow fields with subsonic inlet velocities.[3] Extension of the method to cascades in flow fields of upper transonic region with supersonic inlet velocities, comparison of data, and limitations of the approach are topics discussed here.

Theoretical Considerations

Assumptions

Due to the very complex nature of the real flow in a turbomachine, it is necessary to make some simplifying assumptions about the fluid and the cinematic behaviour of the flow under consideration. Therefore, the following hypothesis are made for the analysis to follow.

- the flow is considered steady relative to the blade
- the flow is two-dimensional
  - the blade-to-blade surface is a surface of revolution
  - the velocity normal to the blade-to-blade surface is zero
- the fluid is nonviscous
- the fluid is isoenergetic
- the velocity magnitude and direction is uniform across the upstream and across the downstream boundaries
- the effects of viscosity are only taken into account to calculate the boundary Layer displacement thickness and the shock/boundary layer interactions
- the vorticity created by the shock wave is ignored herein.

Governing Equations

The basic differential equations of transonic flow are sufficiently well known that a derivation is unnecessary; and, therefore, they will simply be stated in

the form used.

The transonic small disturbance equation is derived as a part of a systematic expansion procedure applied to the exact equations for steady, inviscid, isentropic flow.

continuity eq. $\operatorname{div}(\rho \vec{V}) = 0$ (1)

Euler eq. $(\vec{V}\ \text{grad})\ \vec{V} = -\frac{1}{\rho}\ \text{grad}\ p$ (2)

isentropic rel. $p = k\ \rho^{\gamma}$ (3)

where $\vec{V}$ is the velocity vector, ρ the density, p the pressure, k a constant of proportionality, and γ the ratio of specific heats.

The result is the transonic small perturbation potentiel equation (TPE)[4],[5]

$$(K - (\gamma + 1)\ \phi_x)\ \phi_{xx} + \phi_{\tilde{y}\tilde{y}} = 0 \qquad (4)$$

or alternatively

$$\left(K\ \phi_x - \frac{\gamma + 1}{2}\ \phi_x^2\right)_x + \phi_{\tilde{y}\tilde{y}} = 0 \qquad (5)$$

$$\phi_{\tilde{y}x} - \phi_{x\tilde{y}} = 0$$

with the velocity components u and v in x- and $\tilde{y}$-direction

$$\phi_x = u \qquad \phi_{\tilde{y}} = v \qquad (6)$$

and

$$K = \frac{1 - M_\infty^2}{M_\infty^2\ \delta^{2/3}} \qquad \tilde{y} = (M_\infty^2 \delta)^{1/3} y \qquad (7)$$

The shock jump conditions must be added to the system 5 to form a complet set of equations. However, it turns out that the shock jump conditions are contained in system 5 in the following sense. If their differential equations are integrated across a jump in (u, v), the correct shock relations, to this order, result. That is, each equation in 5 is in conservation form. The corresponding surface integral forms give the shock jump relations

$$\left[K\phi_x - \frac{\gamma+1}{2}\ \phi_x^2\right]\ (d\tilde{y})_s - \left[\phi_{\tilde{y}}\right](dx)_s = 0 \qquad (8)$$

$$\left[\phi_{\tilde{y}}\right]\ (d\tilde{y})_s + \left[\phi_x\right](dx)_s = 0$$

where

$[\ ]$ = jump = $(\ )_{\text{downstream}} - (\ )_{\text{upstream}}$

$(\ )_s$ = element in the shock surface

The two systems of equations 5 and 8 are to be solved numerically for a cascade geometry such as is shown in figure 1 and subject to the following boundary conditions.

Boundary Conditions

The computational domain shown in figure 1, is composed of two channels between three adjacent blades. Upstream and downstream of the blading, as the stream-lines are not known, the periodic boundaries are drawn in the direction of the cord of the profils and fluid is allowed to cross these boundaries. The flow conditions at these boundaries are the same as those at the equivalent lines upstream and downstream of the central profil. Thus they may be adjusted in a correct manner step by step as the solution progresses.

The inlet boundary AB is parallel to the slope of the lower profil's detached bow shock at the upper periodic boundary. Thus its position and inclination must be updated during the iteration process to fulfil the condition of periodicity, too. (The form and position of the detached bow shock is a part of the solution). The outlet boundary is chosen to be sufficiently far away from and parallel to the outlet of the cascade so that the conditions along EF may be considered uniform.

On the rigid boundaries of the profil surfaces the wall tangency condition $\partial\phi/\partial n = 0$ is given in the form :

$$\phi_{\tilde{y}}(x) = F'(x) - i/\delta \qquad (9)$$

where the body shape is given as $\tilde{y}=\delta F(x)$.

If a case with circulation is considered, the Kutta condition that the flow leaves the trailing edge smoothly must be applied. This implies a jump of potential across the x-axis downstream of the profil. This jump is related to the circulation around the airfoil, which is unknown in advance.

These boundary conditions in relation with the transonic small perturbation equation define a presumably unique solution.

Axial velocity ratio

The axial velocity ratio

$$\Omega = \frac{\rho_2\ V_2\ \sin\beta_2}{\rho_1\ V_1\ \sin\beta_1} \qquad (10)$$

has an important influence on the flowfield in a turbomachinery cascade.

With the velocity

$$V = \sqrt{\phi_x^2 + \phi_{\tilde{y}}^2} \qquad (11)$$

the flow angle

$$\sin \beta = \phi_{\tilde{y}} / \sqrt{\phi_x^2 + \phi_{\tilde{y}}^2} \tag{12}$$

and the density ratio

$$\frac{\rho_2}{\rho_1} = \left(\frac{p_2}{p_1}\right)^{\frac{1}{\gamma}} = \left[\frac{1 + \frac{\gamma+1}{2} M_2^2}{1 + \frac{\gamma+1}{2} M_1^2}\right]^{-\frac{1}{\gamma-1}} \tag{13}$$

the small perturbation approximation of the axial velocity ratio becomes

$$\Omega = \frac{\phi_{\tilde{y}2}}{\phi_{\tilde{y}1}} \cdot \left(\frac{p_2}{p_1}\right)^{\frac{1}{\gamma}} \tag{14}$$

$$= \frac{\phi_{\tilde{y}2}}{\phi_{\tilde{y}1}} \cdot \left[\frac{1 + \frac{\gamma+1}{2} M_2^2}{1 + \frac{\gamma+1}{2} M_1^2}\right]^{-\frac{1}{\gamma-1}}$$

During each step of iteration the values of $\phi_{\tilde{y}2}$ are updated according to

$$\phi_{\tilde{y}2} = \phi_{\tilde{y}1} \cdot \Omega/\text{const.} \tag{15}$$

This correction has the effect of a fictitions downstream pressure ($p_{2\ \text{real}} + \Delta p_{2\ \text{fict.}}$) taking into account the pressure-forces on a volume between two non-parallel streamsurfaces (figure 3).

Numerical Solution

Finite Difference Schemes

The mixed differencing relaxation scheme for solving transonic boundary value problems was introduced by Murman, Cole and Krupp to treat the small disturbance formulation for nonlifting and lifting airfoils.(4),(5) Most of our calculations are obtained using unequally spaced grids but in the following, for simplicity, we confine our discussion to evenly spaced grids. More details are given in the cited references.(4)-(8)

The important type-dependent feature of the method is that, in subsonic flow regions central difference operators are used to account for the domain of dependence of elliptic equations. In supersonic flow regions, backward difference operators are used to account for the absence of upstream influence in hyperbolic equations.

For the rectangular grid structure shown in the figures 1 and 2, equation 4 can be approximated using a second-order accurate central difference operator for a point i,j in a subsonic flow region.

$$\left[K - (\gamma + 1)\left(\frac{\phi_{i+1,j} - \phi_{i-1,j}}{2\Delta x}\right)\right] \cdot \left[\frac{\phi_{i+1,j} - 2\phi_{i,j} + \phi_{i-1,j}}{(\Delta x)^2}\right] + \left[\frac{\phi_{i,j+1} - 2\phi_{i,j} + \phi_{i,j-1}}{(\Delta \tilde{y})^2}\right] = 0 \tag{16}$$

The operator is stable by linear stability analysis if the coefficient

$$(\text{Vele})_{i,j} = K - (\gamma + 1)\left(\frac{\phi_{i+1,j} - \phi_{i-1,j}}{2\Delta x}\right) \tag{17}$$

is positiv.

Similarly, an implicit, first-order accurate backward difference operator may be written for a point i,j in a supersonic flow region.

$$\left[K - (\gamma + 1)\left(\frac{\phi_{i,j} - \phi_{i-2,j}}{2\Delta x}\right)\right] \cdot \left[\frac{\phi_{i,j} - 2\phi_{i-1,j} + \phi_{i-2,j}}{(\Delta x)^2}\right] + \left[\frac{\phi_{i,j+1} - 2\phi_{i,j} + \phi_{i,j-1}}{(\Delta \tilde{y})^2}\right] = 0 \tag{18}$$

The operator is stable by linear stability analysis if the coefficient

$$(\text{Velh})_{i,j} = K - (\gamma + 1)\left(\frac{\phi_{i,j} - \phi_{1-2,j}}{2\Delta x}\right) \tag{19}$$

is negativ.

During the iteration procedure $(\text{Vele})_{i,j}$ is computed at each grid point. If $(\text{Vele})_{i,j} > 0$ the flow is subsonic and the elliptic operator (eq. 16) is used. If $(\text{Vele})_{i,j} < 0$ and $(\text{Velh})_{i,j} < 0$, the flow is supersonic and the hyperbolic operator (eq. 18) is used.

As the flow accelerates through sonic velocity from subsonic to supersonic velocities, a point exists where $(Vele)_{i,j} < 0$ and $(Velh)_{i,j} > 0$ and neither equation 16 nor equation 18 is stable. A parabolic difference operator is used for such points.[3]

$$\frac{\phi_{i,j+1} - 2\phi_{i,j} + \phi_{i,j-1}}{(\Delta\tilde{y})^2} = 0 \qquad (20)$$

As the flow decelerates through sonic velocitiy from supersonic to subsonic flow, a point exists where $(Vele)_{i,j} > 0$ and $(Velh)_{i,j} < 0$ and both equation 16 and equation 18 are localy stable. Murman's "shock-point operator" is used for such points. [4]

$$(Vele)_{i,j} \frac{(\phi_{i+1,j} - 2\phi_{i,j} + \phi_{i-1,j})}{(\Delta x)^2} + \qquad (21)$$

$$(Velh)_{i,j} \frac{(\phi_{i,j} - 2\phi_{i-1,j} + \phi_{1-2,j})}{(\Delta x)^2} +$$

$$+ \frac{\phi_{i,j+1} - 2\phi_{i,j} + \phi_{i,j-1}}{(\Delta\tilde{y})^2} = 0$$

Murman has shown that this operator, whose x-differences are the sum of the x-differences of the elliptic and hyperbolic operators, will give the correct weak solution to equation 5. He has further shown that, in the limit of vanishing grid spacing, the correct shock jumps are obtained for oblique shocks when arbitrary grid spacing is used. For shock waves that jump from supersonic to subsonic velocities the jump is spread over three mesh points. When the flow downstream of the shock is supersonic the dissipation errors dominating the first-order accurate hyperbolic operator smear the shock over six to ten mesh points.

The circulation Γ which satisfies the Kutta condition must be obtained as a part of the solution process for ϕ. A cut downstream the central profil is introduced at $y = 0$, $x > 1$ across which the potential jump must equal the circulation Γ. Modified difference operators for $\phi_{\tilde{y}\tilde{y}}$ are written that take into account the jump in ϕ across the cut while maintaining the continuity of ϕ_x and $\phi_{\tilde{y}}$. The standard three point centered difference formulas become

$$(\phi_{\tilde{y}\tilde{y}})_{i,0-} = \frac{1}{\Delta\tilde{y}^2}\left[(\phi_{i,1} - \Gamma_i) - 2\,\phi_{i,0-} + \phi_{i,-1}\right] \qquad (22)$$

$$(\phi_{\tilde{y}\tilde{y}})_{i,1} = \frac{1}{\Delta\tilde{y}^2}\left[\phi_{i,2} - 2\,\phi_{i,1} + (\phi_{i,0-} + \Gamma_i)\right] \qquad (23)$$

The points $(i, 0+)$ are not included in the computation, since $\phi_{i,0+}$ is determined from the computed value for $\phi_{i,0-}$ and the value of Γ_i. The iteration procedure for finding the proper circulation proceeds by choosing an initial circulation Γ_0 from which the outlet-boundary solution is obtained. The circulation at the trailing edge is found from the jump in ϕ. On each iterative sweep of the grid a new value of Γ_{te} is found by linearly extrapolating the ϕ's from above and below. The new Γ_{te} along with Γ_0 is used to determine the Γ_i by interpolation. As the iteration proceeds, new estimates for Γ_0 are made, until a converged solution for ϕ is obtained.

Computational Procedure

In the operation of a compressor cascade with slightly supersonic relative inlet Mach number, it is known that there is a unique incidence associated with the given inlet Mach number.[9] The exit angle depends upon the blade circulation which, in turn, is fixed by the Kutta condition. Thus, neither the inlet nor the exit angle are known a priori for the usual transonic compressor operation. The only independent variables of the flowfield are the inlet Mach number and the static pressure ratio. The problem is then to find the entire flowfield for a given cascade geometry, the inlet Mach number and the static pressure ratio or the inlet-outlet velocity ratio. The inlet and outlet angles must be computed as a part of the solution.

A channel for the flow is defined as shown in figure 1. For subsonic inlet velocities the inlet boundary of the computational domain is taken to be parallel to the inlet of the cascade. The magnitude and direction of the velocity is known there. In the triangle $A\bar{B}B$ the ϕ_x- and $\phi_{\tilde{y}}$- values are constant.

For supersonic inlet velocities the inlet boundary is parallel to the slope of the lower profil's detached bow shock at the upper periodic boundary. Thus, an iterativ process has to be used to specify this boundary as a part of the solution. To find a first guess the form of the detached bow shock is calculated for an isolated profil using Murman's method for the flowfield calculation and Levine's method for the determination of the inlet flow angle.[7],[10] This flowfield is superposed to construct the first approximation of the flowfield in the cascade. The ϕ_x-

and $\phi_{\bar{y}}$ - values of the upper part of the inlet boundary (line 7-B in figure 4) are found by linear extrapolation of those at the boundary A-4, which is equivalent to the bow shock section 6-10. The periodicity of the stand-off distances of the shocks and the distances between the shocks are verified at the periodic boundaries and the grid lines in front of the central profil. Every tenth step of iteration the inlet flow angle is updated. If the inlet-outlet velocity ratio is known the axial velocity ratio is used to determine the exit flow angle. Thus, via the Kutta condition the circulation is prescribed. For a given static pressure ratio, both axial velocity ratio and Kutta condition are necessary to calculate the magnitude and the direction of the flowfield at the outlet.

Results and Comparison with Experimental Data

The method outlined in the foregoing has been applied to the flow through several cascades. The geometries of the cascade, the profils and the inlet and outlet conditions have been chosen so that the results can be compared with experimental data. The profil geometries as well as the cascade data are reported in detail in the references 11a - 12.

To obtain good agreement with the experimental data the boundary layer displacement thickness has been calculated to correct the profil shapes. For the shock boundary layer interaction Melnik's small perturbation approximation of Reshothko-Tucker's theory was used. (13)

Figure 5 shows the computed pressure distribution for a cascade with Do-Al profils. For this low cambered 11 percent supercritical profil excellent agreement has been obtained for subsonic inlet velocities and small deviation angles.

In figure 6 the numerical results for a high cambered, 5.9 percent DCA 48 cascade are compared with experimental data of reference 11b. For the two presented inlet angles the agreement of the results downstream of the shock suffers from the simple shock boundary layer interaction model used.

For supersonic inlet conditions a low cambered, 4.66 percent DCA 9.5 profil with 9.57^{o} camber angle has been chosen. In the figures 7 to 11 results for different prescribed inlet and outlet Mach numbers are compared with the data of reference 11a. The calculated unique incidence for this cascade geometrie is shown in figure 12. The axial velocity ratio used to compute the outlet angles are reported on the graphs.

For shock Mach numbers higher than 1.4 the shock boundary layer interaction is not simulated in a correct manner so that there is a small lack of agreement between experimental data and computed values downstream of the shock. But in general the agreement of the velocity and pressure distribution and the flow angle prediction is rather good.

Conclusion

The transonic relaxation method described has proved to give apparently accurate and usefull results if the non-viscous calculations are combined with a boundary layer calculation. The boundary layer displacement effects must be included to obtain accurate results aft the shock and to eliminate irregularities at the trailing edge. Due to the simple shock boundary layer interaction model used the surface pressure gradients across the shock jumps are slightly steeper than in reality.

The results are obtained using between 1/20 and 1/50 the computer time of the time-dependent methods while avoiding the problem of shock smearing. The extension of the method to three-dimensional flow seems highly promising because of the small CPU-times for two-dimensional cases. Indeed, for wing-body combinations Schmidt and Vanino have already calculated three-dimensional flows using this method. (14), (15).

The major difficulty of the method rests with its restriction to thin, low-cambered profils and in the lack of defining exact locations of oblique shocks. But, with adequate mesh refinement the location of weak oblique shocks may be sufficiently well defined.

Acknowledgment

The auther would like to express his gratitude to Dr. W. Schmidt for helpful discussions during the preparation of this study.

References

1 Wu, Chung Hua, "A general Theory of Three-Dimensional Flow with Subsonic and Supersonic Velocity in Turbomachines Having Arbitrary Hub and Casing shapes. Part I and II, " ASME-Paper 50-A-79, 1950.

2 Katsanis, T., McNally, W., "A Fortran Program for Calculating Velocities and Streamlines on a Blade-to-Blade Stream Surface of a Tandem Blade Turbomachine" NASA TN D 5044, 1969

3 Dodge, P.R., "The Use of a Finite Difference Technique to Predict Cascade, Stator and Rotor Deviation Angles and Optimum Angles of Attack" ASME Paper 73-GT-10, 1973

4 Murman, E.M., Cole J.D.,"Calculation of Plane Steady Transonic Flow", AIAA-Paper No 70-188, Jan. 1970

5 Krupp, J.A., Murman, E.M., "The Numerical Calculation of Steady Transonic Flows Past Thin Lifting Airfoils and Slender Bodies", AIAA-Paper No 71-566, Jan. 1971

6 Murman, E.M., Krupp, J.A., "Solution of the Transonic Potential Equation Using a Mixed Finite Difference System", Lecture Notes in Physics, Vol. 8, Springer Verlag, 1971, pp. 199-206

7 Murman, E.M., "Analysis of Embedded Shock Waves Calculated by Relaxation Methods", Proceeding of AIAA Computational Fluid Dynamics Conference, Palm Spring, Ca. July 1973, pp 27-40

8 Sator, F.G., "Détermination de profils de grilles d'aubes pour compresseurs axiaux "transsonique"., Ph. D. Dissertation Ecole Polytechnique Fédérale de Lausanne, Lausanne, July 1976

9 Starken, H., "Untersuchung der Strömung in ebenen Überschallverzögerungsgittern", Ph. D. Dissertation, Rheinisch-Westfälische Technische Hochschule Aachen, Aachen, 1971

10 Levine, P., "The Two-Dimensional Inflow Conditions for a Supersonic Compressor with Curved Blades", Journal of Applied Mechanics, Vol. 24, No 2, 1957

11a Breugelmans, F.A.E., Starken, H.,"The Cascade and Rotor Section Performance of a 9.57° Camber DCA Airfoil" von Karman Institute for Fluid Dynamics Lecture Series 59, May 1973

11b Breugelmans, F.A.E., "The Cascade and Stator Section Performance of a 48° Cambered DCA Airfoil", von Karman Institute for Fluid Dynamics Lecture Series 59, May 1973

12 Heinemann, H.-J., "Experimentelle Untersuchung an Umlenkgittern für Fan-Strahlen, Teil. III Druckverteilungsmessungen". Deutsche Forschungs-und Versuchsanstalt für Luft-und Raumfahrt Bericht No 25175C13, Sept. 1975

13 Melnik, R.E., Grossmann, B., "Interactions of Normal Shock Waves with Turbulent Boundary Layers at Transonic Speeds", Grumman Research Department Report RE-517J, Mar. 1976

14 Schmidt, W., et al., "Some Results Using Relaxation Methods for Two-and Three-Dimensional Transonic Flows", Lecture Notes in Physics, Vol. 35, Springer Verlag, 1975, pp 364-372

15 Schmidt, W., Vanino, R., "The Analysis of Arbitrary Wingbody Combinations in Transonic Flow Using Relaxation Method", Symposium Transsonicum II, Springer Verlag, 1976, pp. 523-532

Figures

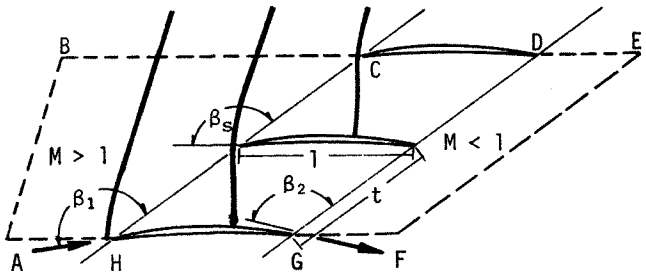

Fig.: 1 Cascade Geometrie and Grid Structure

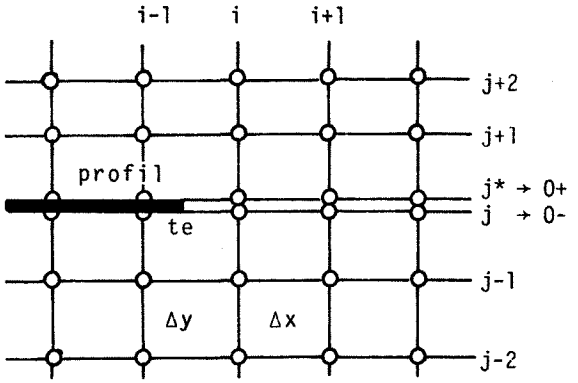

Fig.: 2 Grid Structure and Associated Notation Near the Trailing Edge

Ω	$p_{2_{fictiv}}$	form of the channel reality	calculation
> 1	$>p_{2_{real}}$	$\leftarrow p_2 \rightarrow$	$\leftarrow_{\leftarrow} p_2 + p_{2_{fictiv}}$
< 1	$<p_{2_{real}}$	$\leftarrow p_2 \rightarrow$	$\leftarrow_{\rightarrow} p_2 + p_{2_{fictiv}}$

Fig.: 3 Axial Velocity Ratio

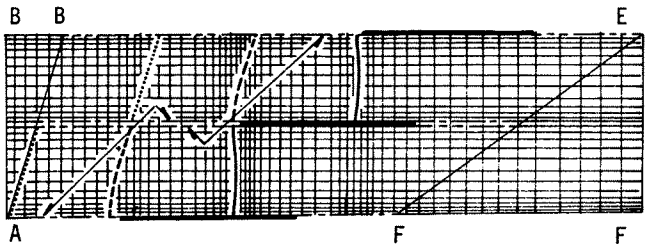

Fig.: 4 Computational Domain and Periodicity

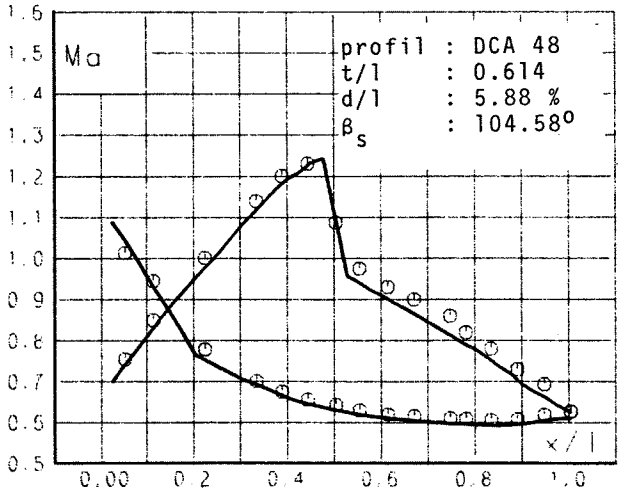

$M_1 = 0.740 \quad \beta_1 = 124.20^0 \quad \Omega = 1.0$

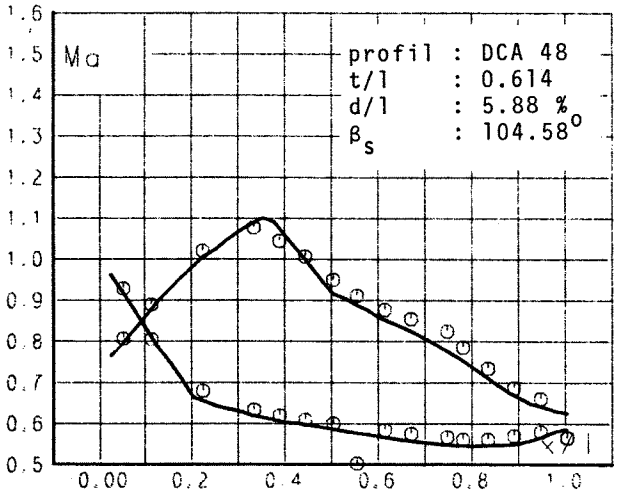

$M_1 = 0.740 \quad \beta_1 = 128.50^0 \quad \Omega = 1.0$

Fig.: 6 Velocity Distribution for the DCA-48-Cascade, Comparison with Data of ref. 11 b

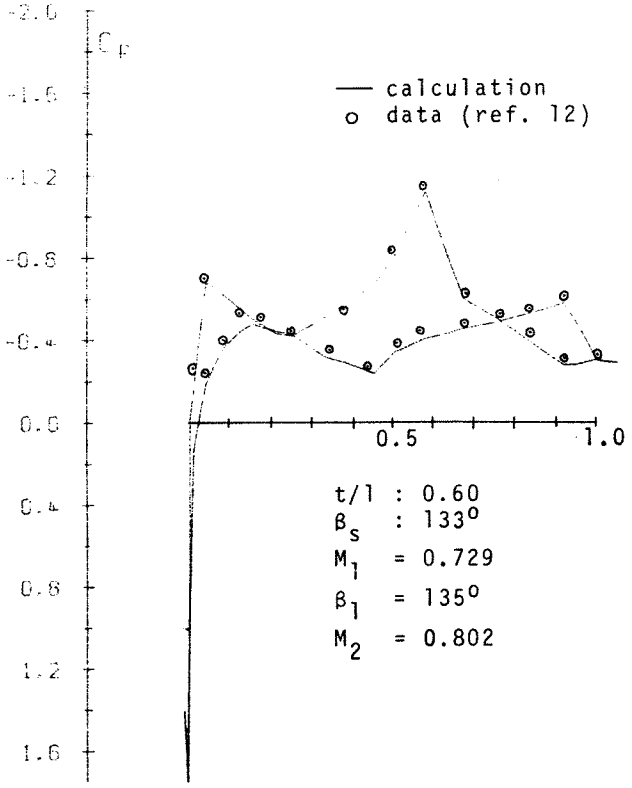

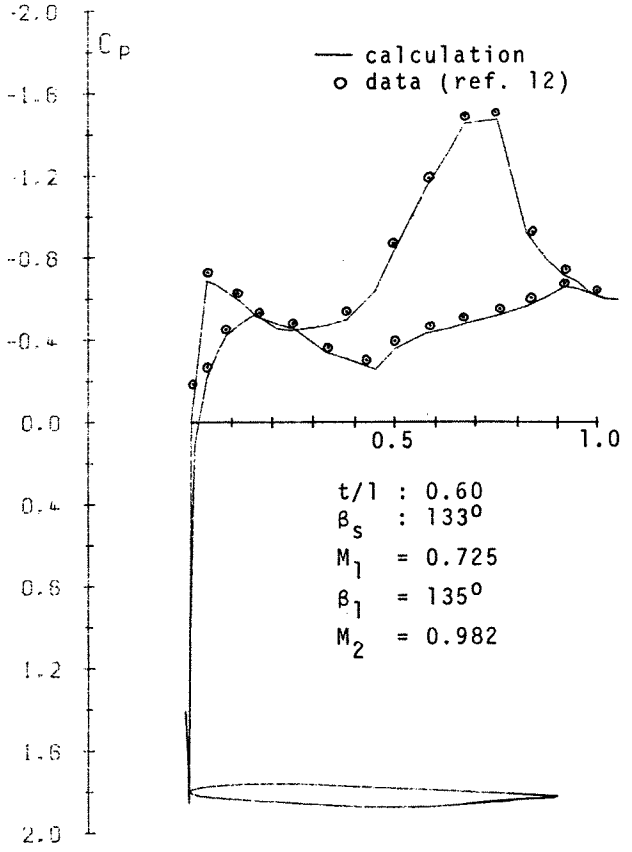

Fig.: 5 Pressure Distributions for the Do-Al-Cascade, Comparison with Data of ref. 12

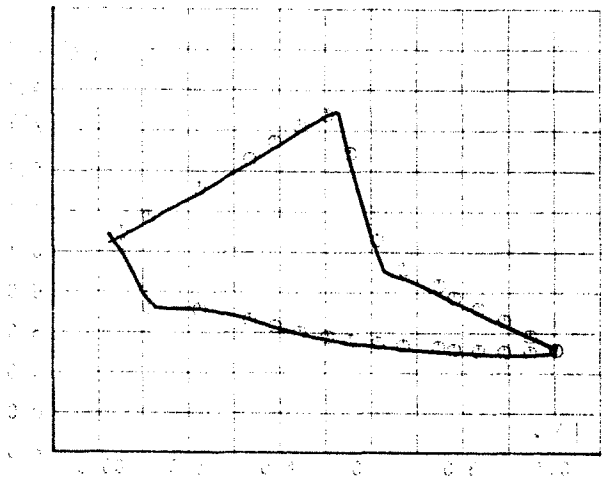

$M_1 = 1.050 \quad M_2 = 0.722 \quad \Omega = 1.154$

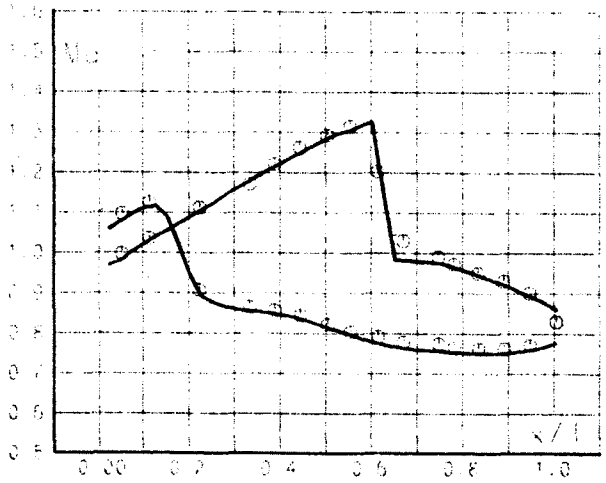

$M_1 = 1.050 \quad M_2 = 0.761 \quad \Omega = 1.145$

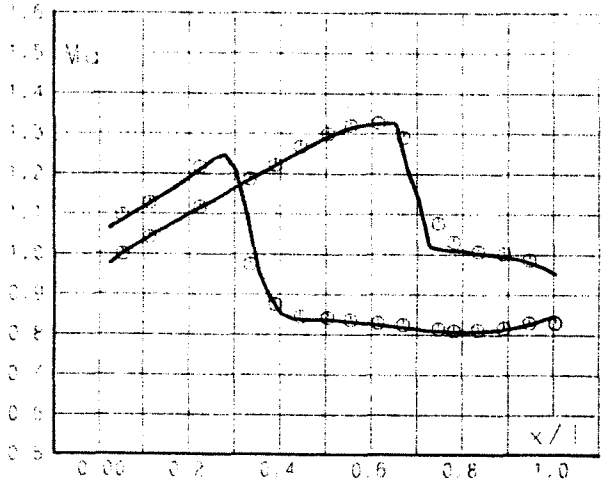

$M_1 = 1.050 \quad M_2 = 0.825 \quad \Omega = 1.147$

Fig.: 7 Influence of the Unique Incidence on the Velocity Distribution. DCA-9.5-Cascade, Comparison with Data of ref. 11a

Geometry of the DCA-9.5-Cascade

Profil : double circular arc

Camber angle	: 9.57°
Maximum Thickness	: 4.66 %
Solidity	: 1.4618
Stagger angle	: 141.35°
Inlet angle (incidence = 0°)	: 146.14°
Outlet angle (deviation = 0°)	: 136.57°

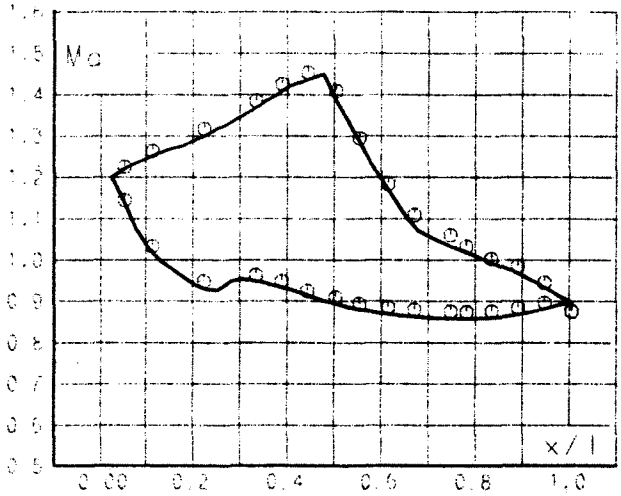

$M_1 = 1.268 \quad M_2 = 0.777 \quad \Omega = 1.168$

Fig.: 8 Velocity Distribution for the DCA-9.5-Cascade, Compariso with Data of ref. 11a

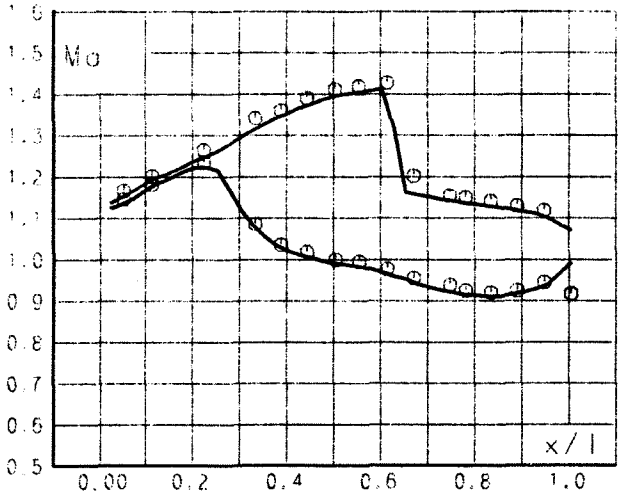

$M_1 = 1.205 \quad M_2 = 0.815 \quad \Omega = 1.061$

Fig.: 9 Velocity Distribution for the DCA-9.5-Cascade, Comparison with Data of ref. 11a

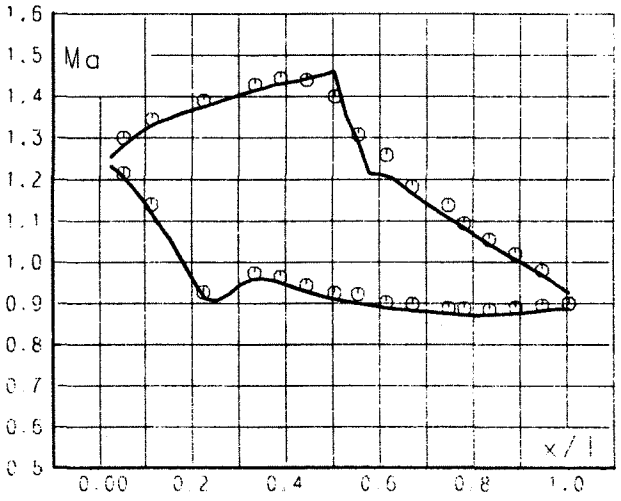

$M_1 = 1.335 \quad M_2 = 0.794 \quad \Omega = 1.208$

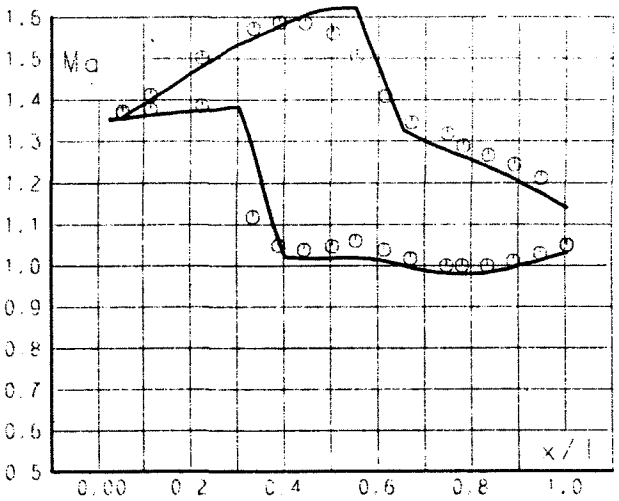

$M_1 = 1.409 \quad M_2 = 0.927 \quad \Omega = 1.165$

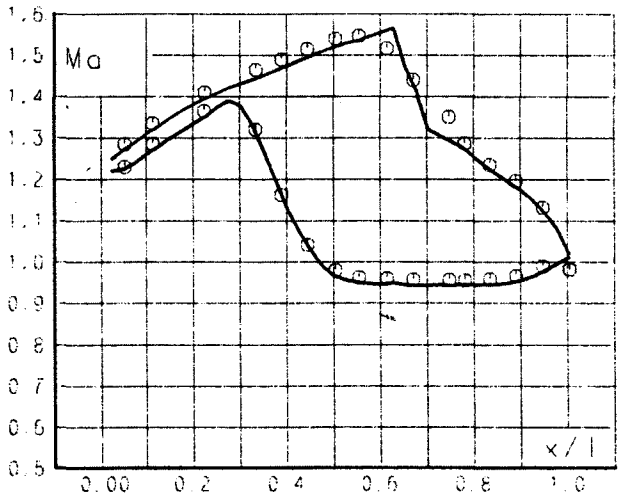

$M_1 = 1.335 \quad M_2 = 0.851 \quad \Omega = 1.149$

Fig.: 10 Velocity Distribution for the DCA-9.5-Cascade

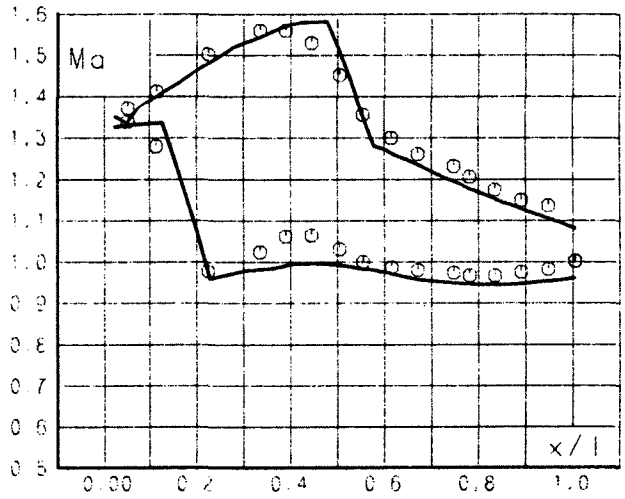

$M_1 = 1.409 \quad M_2 = 0.984 \quad \Omega = 1.282$

Fig.: 11 Velocity Distribution for the DCA-9.5-Cascade

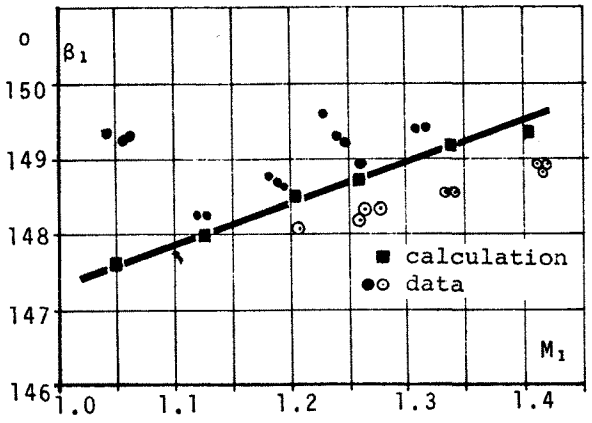

Fig.: 12 Unique Incidence for the DCA-9.5-Cascade (data: ref.11a)